Eq. (25)? Neither of these questions can be answered definitely. However, at $B=10$ Mev the number of b^0 decays observed should have been 15. This estimate could easily be in error by a factor of two, and the frequency of observation of pions in τ' decay in the upper bins also could be in error for statistical or even systematic reasons. We conclude that we cannot exclude the existence of a b^0 of 10-Mev binding energy from the present τ' decay data.

Case III ($B>10$ Mev). The energies of the decay π^+ in $\tau^+ \rightarrow b^0+\pi^+$ decay become greater as the b^0 mass decreases, until finally at about $B=15-20$ Mev the decays would be kinematically distinguished in nuclear track plate experiments. The estimate of Eq. (25) becomes increasingly less reliable as B increases, also, but it is still expected that as B increases, so will the fraction of τ decays going by the b^0 mode. We conclude that the binding in the b^0 is less than 20–30 Mev on the basis of the fact that too few (~ 2) π^+ from decays[14,16] apparently like τ' decay have been found with energies greater than the end point energy of 53 Mev.

ACKNOWLEDGMENTS

We are indebted to Professor F. J. Belinfante and many of the rest of our colleagues of the Purdue Physics Department for helpful and provocative discussions.

[16] These events are discussed by K. Hiida, Nuovo cimento **13**, 1117 (1959).

PHYSICAL REVIEW VOLUME 121, NUMBER 6 MARCH 15, 1961

Cloud-Chamber Study of Hard Collisions of Cosmic-Ray Muons with Electrons*

R. F. Deery† and S. H. Neddermeyer
Department of Physics, University of Washington, Seattle, Washington

(Received November 1, 1960)

The energy distribution of the secondary electrons produced in targets of carbon or paraffin by the μ-e scattering process for muon momenta in the range 5–50 Bev has been measured for electron energies up to 10 Bev, or c.m. momentum transfer up to 100 Mev. A vertical array of three cloud chambers immersed in a magnetic field of 11 000 gauss was used with a fourfold coincidence system. Two flat rectangular proportional counters, suitably biased, together with two Geiger-Müller trays, provided fair rejection of uneventful penetrating particles and a high efficiency for selection of the narrow electronic showers characteristic of the high-energy electromagnetic events. On 5900 counter triggered photographs there were 291 accepted events, having one or more ($\pm$) electrons with energy ≥ 0.10 Bev, believed to originate in μ-e collisions in the (carbon or paraffin) target above the top chamber, from incident muons in the momentum interval 5–50 Bev. The data are compared with a calculation based on the Bhabha formula for spin $\frac{1}{2}$ muons, taking into account the momentum distribution of the incident muons, the energy loss and shower development in the target and the chamber walls, and a theoretical efficiency factor. Arguments are given to show that direct pair production and bremsstrahlung of the muons in the target and in the Pb shield above the apparatus produce negligible effects. The experiment permits a reliable measurement of only the relative distribution. When arbitrarily normalized, the calculated distribution is in fairly good agreement with the data, except for a small systematic difference suggesting an excess of observed events for the harder collisions. Although the discrepancy is interpretable as a statistical fluctuation, the data are fitted much better over the entire range when the basic cross section is modified by a "form factor," F^2 (*greater* than unity), with $F=1+|q^2|\lambda_\mu^2$ where q is the invariant of the 4-momentum transfer in units of $\hbar$, and λ_μ is the Compton wavelength of the muon. This may be the first indication of a deviation from standard quantum electrodynamics for hard μ-e collisions. More strongly it shows that, if there is a deviation, it is not representable by a form factor less than unity.

I. INTRODUCTION

THE essential content of this paper may be appreciated from the Abstract, the plots of the results in Sec. IV, and the conclusions, Sec. VI. The background discussion in the introduction is long because the experiment is really an old one which may have new and interesting aspects. Section II includes the design, the experimental conditions and "boundary" data, with a general discussion of the problems of analysis of the results; Sec. III, apparatus details, calibration and measurement procedures; Sec. IV, the results; and Sec. V, details of the analysis.

Background

The production of high-energy secondary electrons by close collisions of cosmic-ray particles with atomic electrons was one of the first processes to be studied extensively in cosmic rays,[1] and together with other studies, ultimately led to the discovery of the muon.[2] Although the early mistaken but generally believed

* This work has been supported by the Office of Naval Research. An account of it is given in the doctoral thesis of the junior author: R. F. Deery, thesis, University of Washington, 1960 (unpublished).

† Now at the California Institute of Technology, Pasadena, California.

[1] C. D. Anderson and S. H. Neddermeyer, *Proceedings of the International Conference on Physics, London, 1934* (Cambridge University Press, Cambridge, 1934), p. 171.

[2] S. H. Neddermeyer and C. D. Anderson, Phys. Rev. **51**, 884 (1937); Phys. Rev. **54**, 88 (1938); Revs. Modern Phys. **11**, 191 (1939).

(by most theoreticians[3]), identification of the cosmic-ray mesons with the nuclear force meson of Yukawa[4] was from the beginning contradicted by extensive experimental data on the penetrating power of the sea-level particles, there has always remained the residual question whether the muon has any strong interaction other than the normal electromagnetic one. Given a source of high-energy muons there are only three possibilities with present technology for detecting such strong interactions: One is by rapid decay into other particles, which of course is not observed, and the others are by hard collisions with electrons or with nucleons. The experiment of Conversi *et al.*,[5] which finally gave the most conclusive proof that the muon could not be the nuclear force meson, does not exclude the possibility that there may be another kind of short-range interaction. The same is true of all the other elegant and precise experiments which have been done with mu mesonic atoms,[6] which show that to high accuracy the muon has the normal Dirac moment and otherwise behaves as would be expected of a normal Dirac particle whose only strong interaction is electromagnetic. There have been, nevertheless, some slight indications of anomalous behavior.

The experiments on the electron secondaries[1,2] provided the first powerful argument that the bulk of the sea-level particles could not be as heavy as protons, but otherwise made no very penetrating test of theory, especially of the spin-dependent terms or of a possible deviation from theory for very hard collisions. The later experiment by Walker[7] came closer to such a test, and although it might be regarded as giving a suggestion of too many events at large transfers, it was in the main a further verification of the theory for somewhat harder impacts, while still making no critical test for very close collisions.

The ion chamber burst experiments by Schein and Gill[8] provided, in the hands of Christy and Kusaka,[9] an indirect test of the bremsstrahlung process up to several hundred Bev, as well as the first indirect measurement of the muon spin. A recent reanalysis[10] of the Schein and Gill, and later[11] measurements yields a theoretical distribution for spin $\frac{1}{2}$ which fits the experimental data rather closely, hence presumably provides a somewhat more critical test of the bremsstrahlung process for muons up to the 100-Bev region. Since the expected contribution of the μ-e collisions is relatively rather small, the observations give a much less critical test for that process. Observations of the above kind, together with the correlation between the observed spectrum and the underground penetration of the muons,[12] would seem to be fairly stringent tests of the electromagnetic processes of the muons up to very high energy. Yet they are indirect, involving several stages of complicated calculations and numerous corrections and uncertainties. Impressive as the results may be, there is no adequate substitute for experiments in which one comes as close as possible to direct observation of the primary event itself.

The experimental situation with regard to the scattering of muons on nuclei is perhaps more obscure. Most of the work on this problem has been done with sea-level cosmic-ray mesons and has tended to indicate the presence of a tail of large angle scattering,[13] which might require the assumption of a short-range force other than the normal electromagnetic one. Our own less extensive experiments have indicated a somewhat smaller anomaly, which, however, has now been shown to be attributable to errors. A much more definitive experiment has been performed by Masek *et al.*[14] of this laboratory, using 2-Bev muons from the Berkeley bevatron, which shows that the scattering is normal for momentum transfers as high as 400 Mev/c. This does not, however, rule out the possibility that such an anomaly might exist at much higher particle momenta (or momentum transfers) and says nothing about the interesting question of the muon-electron interaction.

Aims

The present experiment is part of a more general re-examination of the supposedly well-known electromagnetic interactions of the muons in hard collisions but under more extreme or better defined experimental conditions than previously achieved. The immediate aim of the muon-electron experiment can be stated as a test of existing theory for harder collisions than previously observed. In collisions for which the invariant of the 4-momentum transfer $|q|>M$, where $M=0.1$ Bev is the muon mass, the particles penetrate to a separation of the order of the Compton wavelength of the muon and for such collisions or harder there may be no firm basis for expecting the normal theory to hold.[15] The energy transfer to the electron, initially at rest in the laboratory system, is $W=|q|^2/2m$, where m is the electron mass. Thus $w=10$ Bev for $|q|=0.1$

[3] See Appendix note 1.
[4] H. Yukawa, Proc. Phys.-Math. Soc. Japan **17**, 48 (1935).
[5] M. Conversi, E. Panchini, and O. Piccioni, Phys. Rev. **71**, 209 (1947).
[6] For example, V. L. Fitch and J. Rainwater, Phys. Rev. **92**, 789 (1953); also, R. L. Garwin, D. P. Hutchinson, S. Penman, and G. Shapiro, Phys. Rev. Letters **2**, 213, 516 (1959).
[7] W. D. Walker, Phys. Rev. **90**, 234 (1953).
[8] M. Schein and P. S. Gill, Revs. Modern Phys. **11**, 267 (1939).
[9] R. F. Christy and S. Kusaka, Phys. Rev. **59**, 405 (1951).
[10] M. R. Gupta, Nuovo cimento **7**, 39 (1958); I. X. Ion, N. J. Ionescu-Pallas, C. C. Potoceanu, Nuovo cimento **9**, 507 (1959).
[11] R. E. Lapp, Phys. Rev. **69**, 321 (1946).
[12] P. H. Barrett, L. M. Bollinger, G. Cocconi, Y. Eisenberg, and K. Greisen, Revs. Modern Phys. **24**, 133 (1952).
[13] We refer only to the review article by G. N. Fowler and A. W. Wolfendale, *Progress in Elementary Particle and Cosmic-Ray Physics* (Interscience Publishers, New York, 1958), Vol. IV, Chap. 4.
[14] G. E. Masek, L. D. Heggie, Y. B. Kim, and R. W. Williams (to be published).
[15] S. D. Drell, Ann. Phys. **4**, 75 (1958). The basic theoretical questions involved in this experiment have been discussed at some length by R. F. Deery [thesis, University of Washington, 1960 (unpublished)].

TABLE I. Summary of target conditions.

	Experiment *A*		Experiment *B*	
	Target	Cloud chamber wall	Target	Cloud chamber wall
Material:	carbon	steel (nonmag.)	paraffin	aluminum
Density: g/cm³	1.30	7.87	0.88	2.70
g/r.l. cm²	44.6	14.1	64.8	24.5
electrons/r.l. cm²	1.35×10^{25}	0.392×10^{25}	1.62×10^{25}	0.712×10^{25}
Thickness: g/cm²	23.1	6.19	17.0	2.42
r.l.	0.521	0.439	0.359	0.099
electrons/cm²	0.701×10^{25}	0.172×10^{25}	0.582×10^{25}	0.0705×10^{25}

Bev, and the incident muon momentum required for this [Sec. V, Eq. (3)] is 17 Bev. The experiment itself is, therefore, an attempt to measure the energy distribution of the secondary electrons produced by direct collisions of muons with atomic electrons clear up to the maximum transferable energy, including as well, measurement of the momenta of the individual muons. The ideal end is to some extent frustrated by shower development in the target (and other difficulties, see Sec. II); nevertheless, a reasonable compromise can be achieved by limiting the target thickness to about 0.5–1.0 radiation lengths and using low atomic number material to maximize the number of electrons per radiation length.

II. THE EXPERIMENT

Design

The experiment was performed in two parts, *A* and *B*, with somewhat different target conditions which are summarized in Table I. A vertical section, Fig. 1, shows the essential features of the experimental arrangement. There are two principal difficulties in the design of the experiment: One is with the target, mentioned above, which arises from the conflict between getting a sufficient yield of events and still making unambiguous identifications; the other is that the necessity for counter discrimination against unaccompanied particles introduces an inaccurately known energy-dependent efficiency factor which increases the difficulty of interpretation and contributes to the uncertainty of the absolute normalization. Arguments are given in Sec. V that the efficiency saturates rather quickly with increasing energy, hence should not seriously distort the observed energy distribution; however, the normalization remains unreliable.

Events were selected by a fourfold coincidence of two *GM* counter trays with two proportional counters of flat geometry. The latter were designed especially for the purpose of permitting efficient selection of the very close pairs or groups of particles which are characteristic of the electromagnetic processes at high energy. The first proportional counter was placed between the target and the top of the upper cloud chamber and was biased to about 1.5 times the pulse height for a "minimum ionization" particle as defined by a point on the knee of the curve of counting rate vs discriminator setting. This was sufficient to discriminate rather strongly against unaccompanied muons, while giving essentially 100% acceptance of muons accompanied by one or more electrons. In about the first half of experiment *A* the top counter was instead placed above the target and used in anticoincidence to insure only one particle going into the target. This was abandoned as it rejected too many true events, and we felt sufficiently sure that false events from the shield could be recognized and rejected. (The foregoing is responsible for an apparent discrepancy in Table II.) A 1.25-cm Pb plate in the bottom of the upper chamber is presumed to identify the secondaries as electrons by their catastrophic energy loss or cascade multiplication. The second proportional

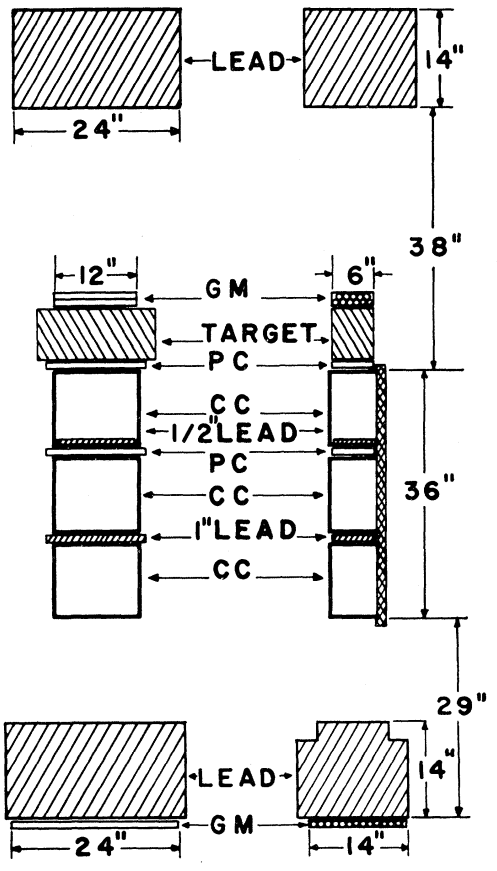

FIG. 1. Section drawing of experimental arrangement.

counter, placed in the channel between the top and middle chambers, was biased slightly higher to about twice minimum to give stronger rejection of singles, but still accept two or more with certainty. A large Geiger-Müller tray placed 75 cm below the bottom of the chamber assembly, under a 35-cm Pb absorber, and a smaller double tray placed on top of the target, with one or more counters being required to trigger in each tray, complete the coincidence system. The function of the 2.54-cm Pb plate between the middle and lower chambers is a further check on the character of the primaries and the conversion of any high-energy photons that may have escaped from the first plate. A 35-cm lead filter is placed above the entire arrangement to remove the incident electromagnetic component and remove or partially convert the strongly interacting component by meson production. Such showers, the so-called penetrating showers, are always easily recognizable and cause no confusion. These, as well as any electronic showers originating in the lead shield, might have been rejected by suitably biased anticoincidence counters; however, the alternative was chosen to leave a 75-cm space between the lead shield and the target to permit the fringing field of the magnet to deflect such particles sufficiently not to be confused with those originating in the target. The main source of possible confusion arising from the presence of the lead shield lies in the photons produced in the last radiation length or so of the lead, either by direct bremsstrahlung of the muons or of shower electrons, and which escape to get converted in the target. They are, in general, emitted at such small angles that their products in the target could easily be confused with true target events of the muons (or *their* higher order products). This source of confusion cannot be averted by any simple system of anticoincidence counters between shield and target. Arguments will be given that the difficulty is not serious.

Analysis of the Results: General

The basic "boundary" data of the experiment are summarized in Table II. Although the muon momenta are measurable in individual cases (after but not before the event!), the use of counter-selected events requires that the data be compared with an indirect analysis using an assumed incident muon spectrum. The analysis is further complicated by the stochastic character of the processes following the initial event, which makes it impossible to trace the electrons back to their origins or to know their initial energies. If the basic data of the experiment are taken to be the measured momenta of the muons and their associated secondaries, together with various judgements exercised as to the character of the events, then the anslysis consists in carrying out an integral over: (a) the assumed cross section, which depends on the energy, w, of the event and the energy E_μ of the incident muon; (b) the assumed energy spectrum of the incident muons; (c) the probability that, given an electron of energy w, formed at height y in the target, an electron of energy E in dE will emerge below, and finally over the thickness of the target. The result then has to be multiplied by an energy dependent selection efficiency factor. The details are given in Sec. V.

TABLE II. "Boundary" data.

	Exp. A	Exp. B	Total
Sensitive time, hours	930[a]	790	1720
Number of muons ±15% in 5–50 Bev	38 850[a]	53 700	92 250
Number of photos	2919	2990	5909
Total accepted events with an $E \geq 0.10$ Bev[b]	131	160	291
Muons (in 5–50 Bev) per hour	41.8	68.0	53.6
Photos/hour	3.14	3.78	3.44
Accepted events/hour	0.141	0.202	0.169
Photos/(muon in 5–50 Bev)	0.0751	0.0556	0.0642
Events/(muon in 5–50 Bev)	0.00337	0.00298	0.00315

[a] The apparent discrepancy between A and B in muons/hour is explained in the text.
[b] Here E refers to the observed energies of individual negatons or positons.

Since the muon momentum is measurable up to about 50 Bev, and since the main interest is in hard collisions, it is convenient to base the analysis on a limited range of muon momentum, 5–50 Bev. Both limits are to some extent arbitrary. The use of the limits simplifies the theoretical interpretation, but entails some experimental uncertainties arising from errors in the measurement of the muon momentum. The muon momentum is measured only after the event; hence, the incident momentum has the additional uncertainty of the estimated event energy. Actually only a lower limit to the incident muon energy was obtained by adding the total "visible" event energy entering the top chamber in the form of positive and negative electrons, an approximation that can have little effect on the main results. The distribution of secondary electrons up to 10 Bev is furthermore not very sensitive to the upper cutoff of the muons. Most of the events whose interpretation is uncertain are in the region of very high incident energy, and it is in this (rejected) region that the lead shield introduces the greatest uncertainties.

III. EXPERIMENTAL DETAILS

Cloud Chamber and Magnet

The chamber is built in three separate sections 27 cm high×37 cm wide×15 cm deep, having a common back plate and common expansion valves extending the full length of the array on either side, but with independently adjustable expansion ratios. The whole array is 91 cm high with 3.2-cm channels provided between chambers for insertion of counters and absorbers. There are a few novel features which are irrelevant and need not be described here. The essential conditions of operation are summarized in Table III. The chamber is enclosed

in a $\frac{1}{8}$-in. thick copper box with side windows against which the lamps are mounted. The box extends through the open front magnet pole nearly to the camera, and that end is uncovered. There are 16 parallel water circuits of $\frac{3}{8}$-in. copper tubing sweated to the outside of the box, through which water is circulated at 20 gal/min. A servo-driven variac regulates a heater which keeps the down-stream thermostat at a constant temperature ± 0.005°C. An auxiliary control, using a point in the copper box as a reference, cools the bottoms of the chambers by circulating water whose temperature is controlled to 0.1 ± 0.01°C below the box temperature. (The latter was on for the second half of the experiment.)

The illumination is produced by two xenon-filled quartz lamps, one on either side of the chamber, which are discharged with 2200 joules each at 3500 volts. The camera views the chamber through the open front pole from a distance of 2.3 m. A single 191-mm 1C Tessar lens is used together with a stereo attachment which places the two chamber images side by side on 70-mm film. An identical system is used for projection, and all track analysis is done either in the reprojection space, or else in nonstereo projection on a screen tilted to lie in the central plane of either chamber image.

The magnet consists of two horizontal rectangular yokes made of forged bars 1 ft×2 ft in section. The yokes are spaced vertically by 3-ft high blocks of iron 1 ft thick which also carry the front and rear poles. The front one has a 1-ft×3-ft opening for photography. The coils have 8000 ft of 1-in. square aluminum tubing with a $\frac{3}{8}$-in. diam round hole for water cooling. They are wound in double pies to put all electrical connections on the outside and to permit parallel water flow from the inside out. The 35-ft lengths were joined by a solid butt weld, after which the hole was drilled out with an extension drill. The welds were then planed down so that they were almost undetectable. There are 480 turns; the front and rear coils are driven by separate generators at 1075 amp and total power 135 kw.

Field Calibration

The magnetic field was calibrated by two independent methods: The first was by a standard induction fluxmeter with which the longitudinal component was measured at 2-in. spacings on a cubical lattice through the volume of the chamber. The second was by means of a series-connected vertical array of 15 pairs of fine copper wires suspended in each chamber, all stretched to the same tension by identical weights and carrying the same, accurately controlled, current. The wires were photographed and their curvatures measured by the same procedures as for measuring tracks. For comparison the lattice measurements were used with interpolation to find the expected integrated deflections of the wires in the second set of measurements. The results agreed to about 1%. Then the wire measurements were used to prepare tables for conversion of curvature to momentum for tracks in various parts of the chamber which are parallel to the chamber face. These include depth and magnification corrections, but corrections for motion in the longitudinal direction, when necessary, have to be put in separately. The extreme variation of the magnetic field from back corners to front middle is large, nearly $\pm 15\%$; however, the variation in effective field for a track traversing various parts of one entire chamber is more typically $\pm 5\%$. No elaborate machinery of point by point averaging, making full use of the field calibration, was set up for this experiment. Instead, for electron tracks traversing one chamber, the appropriate field-curvature relation at the center of the track was applied for the entire track or else an interpolation of the wire measurements was used. For vertical tracks in the center of the middle chamber the momentum is given by $cp/r = 0.333$ Bev/meter, corresponding to an effective field of 11 100 gauss.

TABLE III. Cloud-chamber conditions.

Over-all dimensions, observable volume:	36 in.×12 in.×6 in.
Observable vol. excluding spaces between chambers:	33.75 liters
Effective volume used in this experiment:	15 liters
Field, central plane:	11 200 gauss
Cloud chamber filling:	Argon or Ar-He mixture with 70:30 isoprop. alcohol and water
Expansion ratio:	1.07
Time, event to completion of expansion:	0.012 sec
Time, event to photo:	0.07 and 0.120 sec or both lamps at 0.08–0.100 sec

Measurement of Momentum

Since the single-lens stereo attachment has the effect of making the camera see two displaced and slightly rotated virtual objects, the measurements are made entirely in reprojection. In one system the tracks are projected in stereo on a screen having two degrees of freedom to permit alignment of a fiducial (within limits) with the space tangent of the track. The projector has two more degrees for focusing and for translating the track across the field. Curvature is then measured in terms of rotation of the track tangent as a function of distance along the track. For slightly curved tracks traversing the entire three sections of the chamber the correction for motion along the field is small and can be neglected.

In the second system a straight projection is made without the stereo attachment, but the screen has two orientations corresponding to the central plane of the object space for either picture. Depth in the chamber can be measured in terms of distances of the track image from images of fiducial lines ruled on the front glass. Curvature is measured with a curvometer consisting of a bar of Homalite plastic 12 in. long which is bent into a circular arc by the application of a nearly pure bending moment, through two rigid dural arms

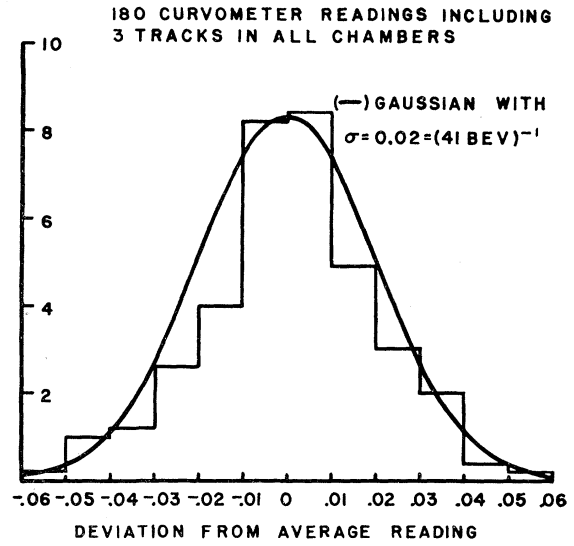

FIG. 2. Curvometer reading error distribution.

clamped to either end. The outer ends of the arms are connected by means of a swivel linkage engaging a right-left screw. The face of the bar which receives the image is painted white, and in the undeformed state is ruled with two closely spaced parallel scratches. To make a measurement the curvometer is laid on the projection table, adjusted to give a best fit to the track, and the curvature is taken from a vernier scale, readable to 0.01 in., which measures the relative displacement of the outer ends of the arms. For not too small radii the radius of curvature in meters is given by $r=2.44/d$, where d is the scale reading in inches, as compared with the relation $r=2.41/d$ calculated in a first approximation from the geometry of the instrument. For central tracks in the plane of the chamber the momentum in Bev is given directly by $p=0.813/d$. The fitting error in $1/p$ has an approximately Gaussian distribution with a standard deviation of about $(45\ \text{Bev})^{-1}$. A composite

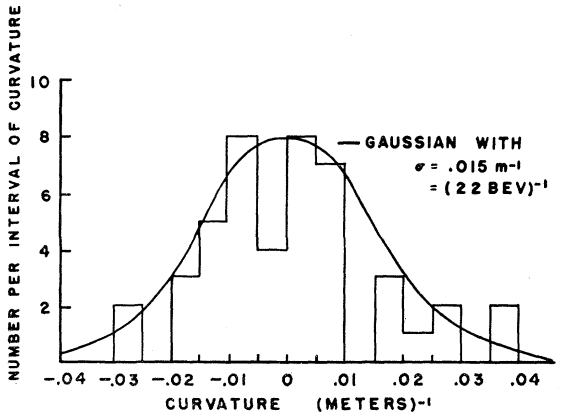

FIG. 3. Curvature distribution of 45 no-field tracks (measured with curvometer).

histogram of the distribution of 180 readings on three tracks is shown in Fig. 2. A distribution of 45 no-field tracks is shown in Fig. 3, compared to a Gaussian of standard deviation 0.015 m^{-1}, or $(22\ \text{Bev})^{-1}$ in terms of equivalent momentum. Since each curvature measurement in the latter distribution is the average of four independent readings, the width represents primarily the distortion error itself for no-field tracks, and $(22\ \text{Bev})^{-1}$ is therefore the most optimistic estimate of the distortion error on tracks measured in a single chamber. The momentum limit for tracks traversing the entire chamber is not well known, but is around 75-100 Bev.

The muons in this experiment traverse the entire length of the three chambers, hence do not deviate by more than 9° from the plane of the chamber face and sense an average field which is typically not far from the central value. The muon momenta were therefore determined from the sagitta of a 32-in. length of track using the mean central field with no correction for motion along the field. Scattering in the lead plates produced a standard error of about ±20% in the sagitta, and the field about ±5% in the momentum. However, the experiment does not depend on the measured muon momenta except near the ends of the 5–50 Bev interval, and the errors can have no appreciable effect on the main results. Electron momenta were measured with the curvometer, using the field value at the center of the track rather than the true effective field. The electrons are ejected at very small angles with the muon tracks; hence, no correction for motion along the field was used. The higher momentum electrons were also measured by the tangent angle method. Those below 400 Mev were outside the range of the curvometer and were measured by fitting to drawn circles.

TABLE IV. Summary of results.

	Exp. A	Exp. B	Total
No. of accepted events (with $E\geq 0.10$ Bev)	131	160	291
No. with dominant positon	13	7	20
Mean No. of (±) electrons per event	1.18	1.10	1.14
No. of *events* having one or more ± electrons with $E>0.5$ Bev	37	56	93
No. of ± electrons with $E>0.5$ Bev	39	58	97
Same, theo. est. $(F=1)$[a]	40	67	107
$(n_\mu^+-n_\mu^+)/(n_\mu^++n_\mu^-)$	0.21±0.09	0.25±0.08	0.23±0.06

Rejected marginal events having at least one ± electron with energy ≥1 Bev:

No. of events	Reason for rejection
2	Probable pair (direct or photon conversion)
1	Wide angle pair
3	$-e$ with doubtful correlation to muon
6	E_μ outside 5–50 Bev interval

[a] The comparison here is not quantitatively meaningful because of the uncertainty in absolute normalization.

IV. EXPERIMENTAL RESULTS

The experimental data are summarized in Table IV. Penetrating pairs and showers and other irrelevant events are not included in the table. The integral distributions of the electrons (No. with energy $>E$) are plotted as a function of E, for experiment A in Fig. 4 and for B in Fig. 5. The accompanying theoretical curves are calculated on the basis of the standard quantum electrodynamics (Bhabha[16] formula) together with an approximate shower theory to give the total number of positive and negative electrons with energy $>E$ expected from the collision events in the target. A composite differential distribution for both A and B is shown in Fig. 6 and the corresponding integral distribution in Fig. 7. The modified theoretical curve (2) is discussed in the next section. For low event energies the momentum distribution of the muons selected by this experiment is expected to be indistinguishable from the total incident spectrum. Figure 8 shows the differential momentum distribution of the muons associated with events with energy <0.6 Bev compared with the spectrum obtained by the Cornell group.[17] The muon spectrum including all μ-e events falls off more rapidly, but will not be discussed in this paper.

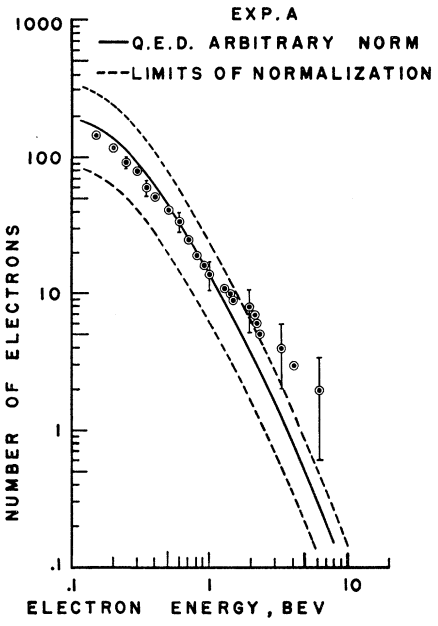

FIG. 4. Experiment A. Integral distribution of ($\pm$) electrons with $E>0.15$ Bev, from 131 events, compared to theoretical calculation based on Bhabha's formula for spin $\frac{1}{2}$ muons. Arbitrary normalization. The rapid decrease in slope below 0.5 Bev arises largely from the event selection efficiency.

[16] H. J. Bhabha, Proc. Roy. Soc. (London) **A164**, 257 (1938); also B. Rossi, *High-Energy Particles* (Prentice-Hall, Inc., New York, 1952), p. 16.

[17] J. Pine, R. J. Davisson, and K. Greisen, Nuovo cimento **14**, 1181 (1959).

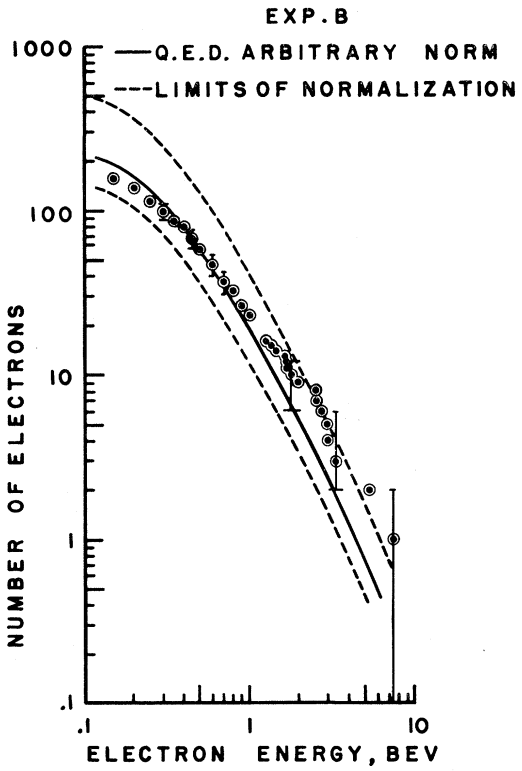

FIG. 5. Experiment B; 160 events.

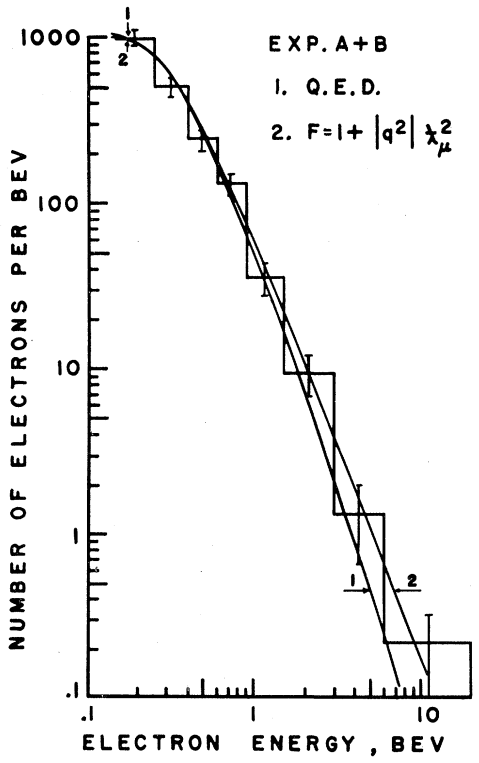

FIG. 6. Composite differential distribution for A and B together. Curve 2 based on cross section modified by factor F^2, where F is the "form factor" shown.

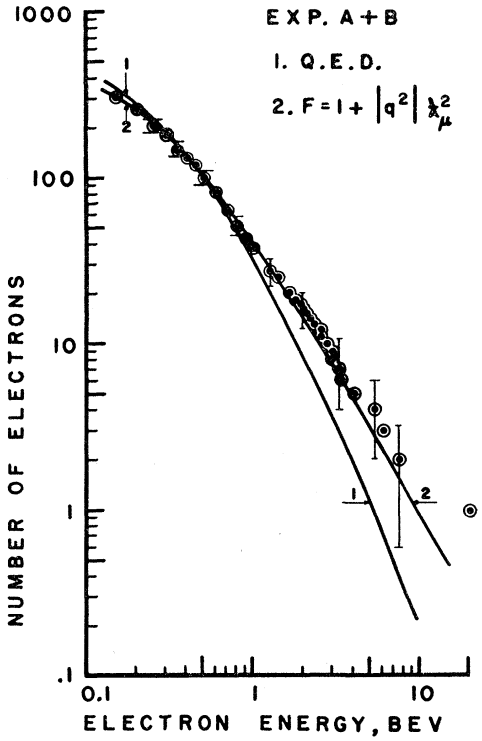

FIG. 7. Integral distributions, equivalent to Fig. 6.

V. ANALYSIS AND DISCUSSION OF RESULTS

The struck electron, in general, will lose energy appreciably by bremsstrahlung before reaching the sensitive volume of the chamber where its trajectory is observed. The resulting distribution of electron energies can be calculated taking into account this effect by folding the bremsstrahlung loss distribution into the collision energy distribution. There is, however, a complication due to the possibility of pair production by the bremsstrahlung or even further shower development giving rise to additional electrons. Therefore, the observable distribution of electron energies must be determined with the aid of some shower theory. Fortunately, the shape of the resulting distribution is not sensitive to these corrections; only the absolute normalization is seriously affected.

None of the many more recent shower theory calculations are applicable to the case of thin layers (less than one radiation length) and do not estimate reliably the distribution of electrons which have a large fraction of the initial energy. Thus, it is necessary to use the original Bhabha and Heitler[18] method to calculate the shower energy distribution. They calculate the number of electrons from each generation in the shower emerging at an arbitrary thickness as a function of emerging energy. For small thickness ($\lesssim 1$ radiation length), the distribution of electron energies greater than a few tenths of the initial energy is given almost entirely by the contribution from the parent electron and its first generation offspring. Later generations in the shower do not have much chance to contribute an energetic electron at a depth of a fraction of a radiation length.

What needs to be calculated is the expected number of electrons $N_{\text{exp}}(E)$ reaching the chamber with energy greater than E as a function of E. The collision electrons are assumed, with negligible error, to be produced with equal probability at all thicknesses above the chamber. The Bhabha-Heitler theory is used to determine the number of electrons entering the upper chamber with energy greater than E, given the initial electron to be produced at height t with energy w. We call this function $n(E,w,t)$, with t expressed in radiation lengths. From it we determine the average shower functions pertinent to the two experiments by a linear average over target

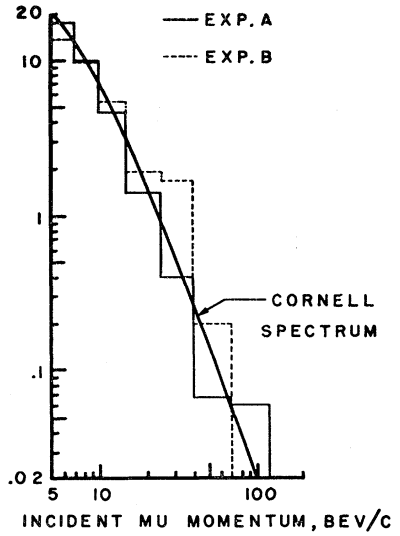

FIG. 8. Observed differential spectrum of selected muons, for event energies <0.6 Bev, including those above 50 Bev which were rejected in the main part of the experiment. Curve shows the Cornell spectrum, which was used in the calculations.

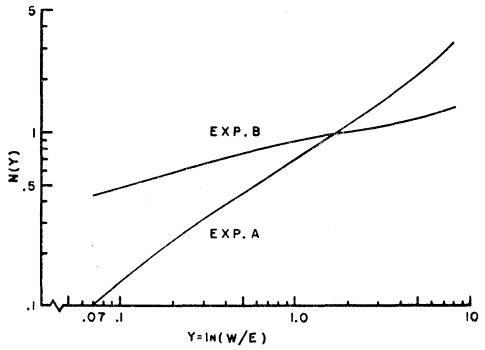

FIG. 9. Plots of the calculated shower functions for experiments A and B. Expected number of observed $\pm$electrons of energy $>E$ when the event energy is w.

[18] H. J. Bhabha and W. Heitler, Proc. Roy. Soc. (London) **A159**, 432 (1937).

thickness. These are called N_A, N_B, for experiments A and B, or typically $N(w/E)$, since they depend on w,E only through the ratio w/E. We have

$$N(w/E)=\frac{1}{\tau_T}\int_{\tau_C}^{\tau_C+\tau_T} n(E,w,t)dt, \quad (1)$$

where τ_T, τ_C, the radiation length thicknesses of target and chamber wall, differ for experiments A and B, but the function n is the same for both.

The functions N_A, N_B are plotted in Fig. 9. The integral energy distribution $N_{\exp}(E)$ in the chamber is then obtained by folding the above functions into the differential production probability $P(w,E_\mu)$ as given by Bhabha,[16] modified by a form factor $F(w)$, and integrated over the muon energy spectrum. Thus:

$$N_{\exp}(E)=2\pi r_0^2 m_e c^2 n_e \int_E^{w_m} dw F(w) N\left(\frac{w}{E}\right) \times \int_{E_1}^{50\ \text{Bev}} \frac{dE_\mu}{w^2}\left(1-\frac{w}{w_m}+\frac{1}{2}\frac{w^2}{E_\mu^2}\right)\frac{dn_\mu}{dE_\mu}, \quad (2)$$

where

$$E_1=5\ \text{Bev} \quad \text{when} \quad E_m(w)\leq 5\ \text{Bev},$$
$$=E_m(w) \quad \text{when} \quad E_m(w)>5\ \text{Bev},$$

and $E_m(w)$ is the minimum muon energy to give an electron the energy w. The latter connection is the same as between E_μ and w_m, given to good accuracy by

$$w_m=E_\mu^2/(E_\mu+m^2/2m_e)=E_\mu^2/(E_\mu+10.9) \quad \text{(in Bev units)}. \quad (3)$$

Since in this experiment $E_\mu>5$ Bev$=50m$, E_μ and p_μ are almost of the same magnitude in energy units.

An indication of the influence of the shower functions is given by comparing the resulting distributions for the two experiments and for the case of no shower correction at all ($N=1.0$). Figure 10 shows these distributions with form factor equal to unity, normalized to one incident muon and with the coefficient of the integral in (2) put equal to unity. These curves indicate that the shower function contributes a normalization factor but no large change in shape in the distribution function.

Since the low-energy data are used to determine the normalization of the theoretical curves, it is necessary to determine the relative efficiency for detecting these events compared to the higher energy ones. The effect of the magnetic field is to curl up low-energy electrons so that they cannot trigger both proportional counters, causing a low-energy cutoff at about 100 Mev. However, this effect results in no loss of efficiency for electrons above 400 Mev.

There is also the efficiency of the counter system to be considered. The prime source of uncertainty is the response of the second proportional counter which is situated under a 1.25-cm layer of lead. This counter was biased at about twice minimum ionization level. The muon must go through this counter, so it should take only one electron emerging from the lead (even as low as 5 Mev) to produce a sufficiently large pulse. Wilson[19] has calculated the shower development of electrons from 50 to 500 Mev in lead by means of a Monte Carlo method. His calculations yield an average number and the distribution in number of emerging electrons with energy greater than 10 Mev. A Poisson distribution based on the average number underestimates the likelihood of pairs of electrons emerging and overestimates the probability for triples. The probability for zero or one is, however, fairly well given by the Poisson. If we assume that one or more electrons (in addition to the muon) will reliably trigger the counter and use the Poisson distribution based on Wilson's results, we obtain an efficiency factor which makes the shape of the theoretical distribution fit the data in the 100- to 500-Mev range remarkably well. If one assumes two or more electrons are required, the resulting efficiency factor falls off much faster below 400 Mev but reaches 90% at 500 Mev. Assuming three electrons are required gives

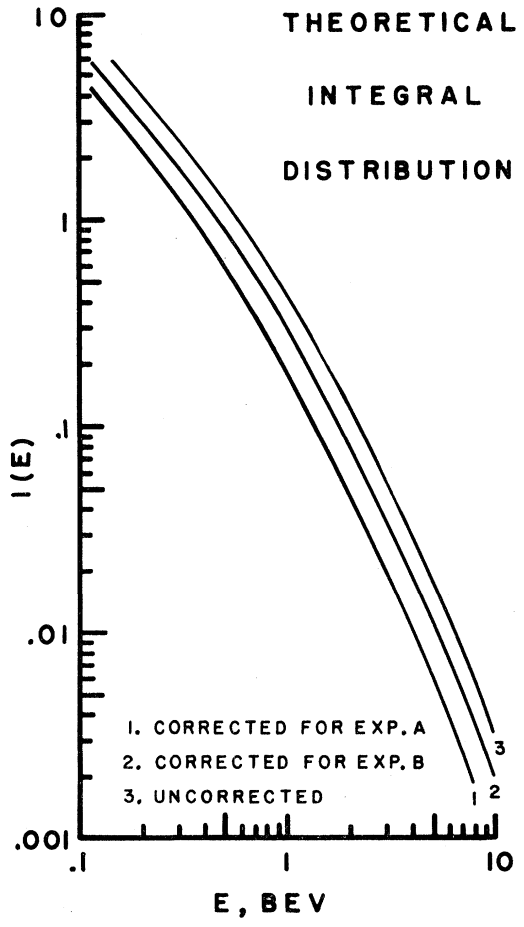

FIG. 10. Shows relative effect of the shower functions on the calculated distributions (without the efficiency factor).

[19] R. R. Wilson, Phys. Rev. 86, 261(1952).

an efficiency correction which causes the theoretical integral curve to level off below 300 Mev in a way quite incompatible with the data. We conclude that the counters were in fact detecting a single electron fairly well. The efficiency factor based on the Poisson distribution for one or more electrons is thus used in correcting the theoretical distribution below 500 Mev.

In the integral distributions, shown separately for Exp. *A* in Fig. 4 and for *B* in Fig. 5, the extreme estimated limits of the normalization are unfortunately rather wide; hence, the actual normalization used is arbitrary. Although the experimental conditions are quite different, the two experiments exhibit a very similar trend in the relation between the data and the curves calculated from the formulas derived from standard quantum electrodynamics (QED). In the composite of the two, shown as a differential distribution in Fig. 6, the difference between the histograms and the curve is not particularly striking; however, the difference is systematic and cumulative, resulting in a rather marked difference in the integral distributions for *A* and *B* separately and in the total shown in Fig. 7. No appreciable part of the difference can be accounted for in terms of errors in the momentum measurements of either the electrons or the muons. The slope of the curves is furthermore largely independent of the way in which the energy losses of the electrons themselves in the target are treated (Fig. 10). A considerably more crude analysis in which fluctuations and showers are ignored and the electrons are treated as undergoing a definite energy loss equal to the mean given by the Bethe-Heitler theory, $-dE/dt=E$ gives a curve which is slightly steeper at the high-energy end. However, to compare with the data in this case, the best one can do is to select the dominant negative electron in each event rather than using all of both signs, and that puts the data still somewhat further from the calculated curve, but with a total discrepancy not much different from that shown in Fig. 7.

We conclude that the discrepancy between the data and the calculated curve cannot be understood either in terms of faulty analysis or errors of measurement. Since the numbers are small, the effect could be explained as a statistical fluctuation.[20] Nevertheless, the difficulty of interpreting the discrepancy in terms of systematic or other errors suggests that one should at least explore other implications of the result. The fact that there is an excess of events at high energy excludes a form factor of a kind representing a simple smearing out of charge. However, the beginning of a "breakdown" of normal QED at high momentum transfers might be represented in terms of a "form factor" *greater* than unity which is a function of $|q^2|$, the invariant of the 4-momentum transfer, but which would not really distinguish between a "breakdown" and a structure effect of the muon.[15] The effect of such a form factor, given by $F=1+|q^2|\lambda_\mu^2$ for F not too much greater than 1, where λ_μ is the Compton wavelength of the muon and q is in units of $\hbar$, on the calculated distribution is shown in curve 2 of Fig. 6 where the Bhabha formula has been multiplied by $F^2(q^2)$. The most impressive fact about the comparison is that it indicates improved agreement with the experimental data over the whole range, not just at the highest energies. Despite the weak statistics at the high-energy end, this may give considerable strength to the argument that the present experiment reveals for the first time substantial evidence for the inadequacy of the standard QED formula for μ-e collisions at distances of the order of 10^{-13} cm.

[20] See Appendix, note 2.

Other Interpretations; Spin Term

The assumption has been implicit throughout this paper that we are dealing with spin $\frac{1}{2}$ particles having the muon mass, and, considering the accumulated body of experimental evidence, it would seem unrealistic to assume otherwise. If the effect of the spin is defined by the difference between the cross section for spin $\frac{1}{2}$ and that for spin 0, the spin term contributes an appreciable number of events at high energy; in fact, it is the only contributing part when w is just below w_m, and accounts for more than half the expected number of 10-Bev events produced in the target by those muons in the range 5–50 Bev. The question of interpreting the data in terms of an admixture of particles of higher spin has not been investigated, although the effect should be in the right direction.

Bremsstrahlung and Direct Pair Production

The effective thickness of the lead shield for the production of bremsstrahlung which escapes to the target is just $1/\kappa$ where κ is the conversion coefficient per radiation length (r.l.). The expected number of pairs resulting from the conversion of such photons in the target is then given by $n_p=(\langle\lambda\rangle/\kappa)(1-e^{-\kappa t})N_\mu$, where $N_\mu\approx 1.0\times 10^5$ is the total number of muons in 5–50 Bev traversing the apparatus, t is the target thickness in r.l. or 0.44, effective, for both experiments together, and $\lambda\approx(m_e/m)^2\ln(E/k)$ is the probability per radiation length in the shield for a muon of mass m, energy E, to produce a photon of energy greater than k. The angular bracket means the average over the accepted part of the muon spectrum for which $E>k$. With the above numbers we get, for $k=2$ Bev, $\langle\lambda\rangle=3.9\times 10^{-5}$ per r.l., and $n_p=1.46$.

For the number of pairs from bremsstrahlung produced *and* converted in the target we have $n_p=\langle\lambda\rangle[t-(1/\kappa)(1-e^{-\kappa t})]N_\mu=0.28$. We thus expect bremsstrahlung from both sources to contribute less than 2 pairs with energy higher than 2 Bev.

Pairs produced in the lead shield may safely be assumed to be eliminated by inspection. For those produced in the target itself, we use the complete shielding

approximation for high-energy pairs as given by Rossi[21] from Bhabha's theory. We integrate over the pair energy and divide by $4\alpha(N/A)Z^2r_0^2\ln(183Z^{-\frac{1}{3}})$ (r.l./gram cm^{-2}) to obtain the probability per radiation length for the production of a pair with energy greater than E by a muon of energy E_μ:

$$P(E,E_\mu)=\frac{\alpha}{\pi}\frac{(m_e/m)^2}{\ln(183Z^{-\frac{1}{3}})}\left(\frac{E_\mu^2}{E^2}-1\right)\ln\frac{2E_\mu}{mc^2}.$$

When averaged over the accepted muon spectrum for $E=2$, we obtain $\langle P\rangle=3.63\times10^{-6}$(r.l.)$^{-1}$ and with the number of muons and target thickness given above we obtain 0.16 pair with energy greater than 2 Bev. The expected number of pairs (>2 Bev) from the above three sources is then about 1.9, and should produce no serious effect on the observed distribution. In fact, two pairs (+11.5, −2.5) and (+1.4, −1.3) were already rejected as probable conversion or direct pairs (the numbers are energy in Bev), but two, more complex, events (−6.1, +3.3, −1.27, +0.06) and (+3.3, −0.83, −0.03, −0.02) were accepted, although they too could have originated as pairs.[22] It should be possible with more detailed analysis of the fluctuation problem to arrive at more clearly defined criteria for acceptance or rejection of events. It seems very unlikely, however, that we have made any bad error. The remainder of the events above 2 Bev have dominant negatons with at most very low-energy showers. There are, however, 14 events altogether, out of the 291, in which there is a dominant positive. This does not seem too unreasonable, although we do not have an estimate of how many should have been expected.

Contamination by Protons and Pions

Contamination by protons and pions must be largely eliminated by the lead shield or be contained in the rejected high-energy events originating mostly in the lead shield. Any residual contamination, if it had any observable effect at all, should presumably give a deficiency rather than an excess of events at high energy.

Positive Excess

The positive excess is usually defined by the parameter $\eta=(n_+-n_-)/(n_++n_-)$. Several experiments by other workers[17] give a mean of about 0.11 ± 0.02 which is roughly independent of momentum over the entire 5–50 Bev range of the present experiment. The result for this experiment is high, 0.23 ± 0.06, with a much larger uncertainty (standard deviation). There is no significant difference between the electron energy distributions from positive and negative muons, and we conclude that, at least for the present, the discrepancy has to be attributed to a statistical fluctuation and a possible small systematic error. To attribute the entire effect to such errors is insupportable, and a small error tending to distort tracks in the positive sense cannot account for the apparent excess of high-energy electrons. The segregated distributions from positive and negative muons are shown in Fig. 11.

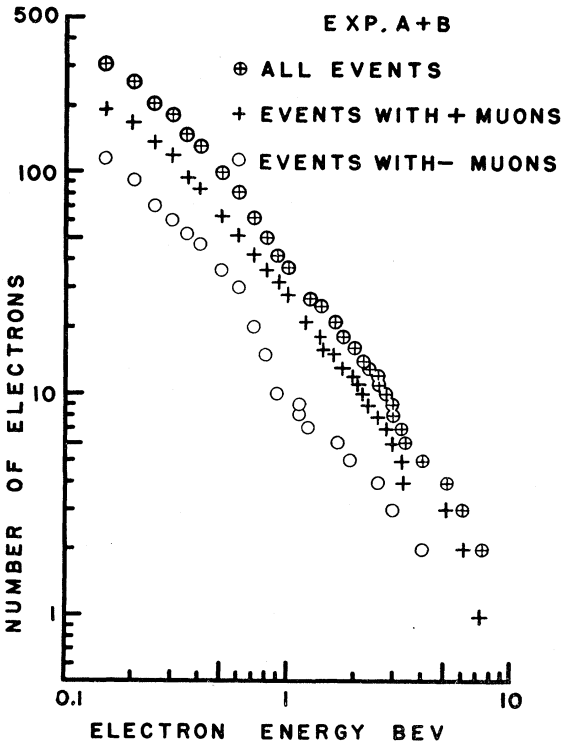

FIG. 11. Observed integral distributions segregated according to sign of the muon.

VI. CONCLUSIONS

The experimental results presented above provide the first substantial evidence for an abnormally large interaction in close collisions between muons and electrons with c.m. momentum transfer up to 100 Mev, or energy transfer to the electron up to 10 Bev in the laboratory system. The conclusion is weakened by the small number of events which makes it impossible to exclude with high confidence the interpretation of the effect as a statistical fluctuation; however, the conclusion is supported by the fact that the results are fitted better over the entire range by a modified QED formula containing a simple relativistically invariant form factor which becomes greater than unity for momentum transfers of the order of $m_\mu c$. The experiment would seem definitely to exclude a form factor which becomes less than one under the same circumstances, corresponding to a simple extended charge distribution. We have not been able to explain the observed effect in terms of random or systematic errors, or in terms of false events produced either by bremsstrahlung or direct pair production in the shield or the target, or by events produced by nucleons and pions.

[21] See Rossi, reference 16, p. 87.
[22] See Appendix, note 3.

ACKNOWLEDGMENTS

We are greatly indebted to Dr. J. H. Manley for his interest and support in the beginning phases of the work and to Dr. W. A. Hane, who was largely responsible for the design and construction of the basic circuitry. The construction of the magnet coil and of the cloud chamber was done mainly under the supervision of E. B. Cottingham who also contributed many useful and ingenious ideas. J. Johnson fabricated the quartz lamps in the local glass shop. Stanley Curtis was of great assistance in running the apparatus and analyzing the data. The junior author (R.F.D.) was supported by a research assistantship under the Office of Naval Research contract, which also provided the main support for the entire program.

APPENDIX

Note 1 (by senior author). This sentence takes issue with a curious and misleading statement by Marshak [*Meson Physics* (McGraw-Hill Book Company, Inc., New York, 1952), p. 202, line 1]. From an experimental point of view the identification of the original mesons with the Yukawa particle was at least regarded as something that had yet to be proved rather than accepted as obvious. [Revs. Modern Phys. **11**, 207 (1939), last paragraph. See also Yukawa's interesting remarks on the muon: Revs. Modern Phys. **29**, 214 (1957).] The discovery of the muon was incidental to the verification of the theory of collisions with electrons for transfers up to 200 Mev and of the bremsstrahlung of electrons up to 500 Mev. The theory of the various electromagnetic processes was a useful link which pervaded many of the arguments. However, it is not to discredit theory or theoreticians to point out that the muon, like the positon, was a purely experimental discovery in the sense that it was made entirely independently of any theoretical considerations of what particles should or should not exist. The same, if not true of the pion, is unquestionably true of the hyperons and K mesons.

Note 2. The perversity of statistical fluctuations in physics experiments is too well known to require comment. However, the excess involves such a small number of particles that one may hardly be justified at all in discussing other interpretations of the results. Thus, if there had been 10 particles instead of 15 above 2 Bev, the discrepancy with the QED integral curve might have been quite unimpressive. The Poisson distribution gives a probability 0.08 for getting 15 events or more when the expected number is 10, and this may be the most optimistic estimate if one is prejudiced to seek a physical interpretation rather than statistical. However, even that argument is weakened by the uncertainty in absolute normalization.

Note 3. The highest energy event recorded (20 Bev "negaton" with 20 Bev "muon") presents several difficulties and uncertainties in interpretation, including that it is the only one in which the secondary apparently has a nuclear interaction in the lead instead of undergoing the normally expected radiative processes. It should probably be rejected. If the two events mentioned (preceding reference 22) are also rejected (and they probably should not be) then the effect is to bring the integral distribution in Fig. 7 down close to the QED curve at the high energy end, but still leave the apparent excess in the middle region.